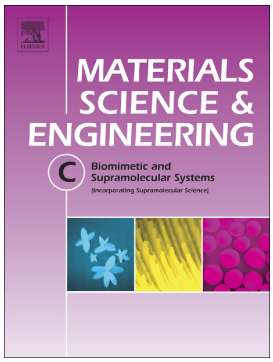

Design of dialdehyde cellulose crosslinked poly(vinyl alcohol) hydrogels for transdermal drug delivery and wound dressings

Monika Muchová, Lukáš Münster, Zdenka Capáková, Veronika Mikulcová, Ivo Kuřitka, Jan Vícha

PII: S0928-4931(20)31246-7

DOI: https://doi.org/10.1016/j.msec.2020.111242

Reference: MSC 111242

To appear in: *Materials Science & Engineering C*

Received date: 22 March 2020

Revised date: 18 June 2020

Accepted date: 24 June 2020

Please cite this article as: M. Muchová, L. Münster, Z. Capáková, et al., Design of dialdehyde cellulose crosslinked poly(vinyl alcohol) hydrogels for transdermal drug delivery and wound dressings, *Materials Science & Engineering C* (2020), https://doi.org/10.1016/j.msec.2020.111242

Design of Dialdehyde cellulose crosslinked poly(vinyl alcohol) hydrogels for transdermal drug delivery and wound dressings

Monika Muchová, Lukáš Münster, Zdenka Capáková, Veronika Mikulcová, Ivo Kuřitka, Jan Vícha*

Centre of Polymer Systems, Tomas Bata University in Zlín, tř. Tomáše Bati 5678, 760 01 Zlín, Czech Republic

ABSTRACT

2,3-dialdehyde cellulose (DAC) was used as an efficient and low-toxicity crosslinker to prepare thin PVA/DAC hydrogel films designed for topical applications such as drug-loaded patches, wound dressings or cosmetic products. An optimization of hydrogel properties was achieved by the variation of two factors – the amount of crosslinker and the weight-average molecular weight (M_w) of the source PVA. The role of each factor to network parameters, mechanical, rheological and surface properties, hydrogel porosity and transdermal absorption is discussed. The best results were obtained for hydrogel films prepared using 0.25 wt.% of DAC and PVA with M_w = 130 kDa, which had a high porosity and drug-loading capacity (high water content), mechanical properties allowing easy handling together with best adherence to the skin from all tested samples and improved transdermal drug-delivery. Hydrogel films are biocompatible, show no cytotoxicity and no negative impact on cell growth and morphology in their presence was observed. Furthermore, hydrogels do not support cell migration and attachment to their surface, which should ensure easy removal of hydrogel patches even from wounded or damaged skin after use.

Keywords: poly(vinyl alcohol); dialdehyde cellulose; transdermal; hydrogel; drug delivery; wound dressing;

1. INTRODUCTION

Hydrogel-based biomaterials receive a steadily growing attention due to their similarity to living tissues in terms of mechanical properties, porosity and high content of water. The last two qualities allow hydrogels to accommodate, store, and later release various substances, making them excellent materials for a wide range of drug-delivery applications in both medicine and cosmetics, i.e. from injectable drug-delivery depots to dermal patches, or from drug-loaded wound dressings to hydrating masks. In contrast to implantable drug depots, topically applied hydrogels could be easily removed and replaced after their content is depleted, which is ideal for sustained, painless, and controlled delivery of biologically active compounds.[1]

Hydrogel films are also excellent wound dressing materials as they naturally hydrate skin and keep the wound zone moist and wettable, which accelerates healing,[2] soothe and cool burns and reduce pain and inflammation.[3] Hydrogels loaded with antibiotics and anti-inflammatory agents can also deliver the active compounds directly to the wounded area, reducing the risk of infection.

Necessary characteristics of hydrogels intended for topical applications include: biocompatibility, large loading capacity (equilibrium water content), good adherence to the skin (bioadhesivity), which increases dermal absorption of compounds loaded in the hydrogel,[4] and mechanical stability sufficient for easy removal. Hydrogels intended as wound dressings should not interfere with the cell growth and formation of new tissues. Simultaneously, they should not support cell migration and attachment to their surface or bulk, which may complicate their removal from the wounded area and lead to the disturbance of tender healing tissue.

To successfully balance all these qualities is not an easy task. For instance, purely biopolymer-based hydrogels often have poor mechanical properties in the swollen state, which make them difficult to handle and to remove from skin. Hydrogels based on artificial polymers have well-defined structure and properties but may suffer from other disadvantages. For instance, hydrogels based on poly(vinyl alcohol), PVA, are used for preparation of immunotherapeutic anticancer gels and transdermal patches, [5,6] wound dressings,[3] drug-delivery patches[7] and contact lenses.[8] However, properties of PVA hydrogels are difficult to optimize – they tend to have poor elasticity, high stiffness and relatively low hydrophilicity. Possible solution is to use hybrid hydrogels composed from two polymers of both natural and artificial origin.[3] Properties of hybrid hydrogels are generally better defined than in case of purely biopolymer-based analogs and their individual attributes can be more easily optimized than those of synthetic polymer-based hydrogels.

In this work we investigate hydrogel films composed of PVA crosslinked by 2,3-dialdehydecellulose, DAC, which is prepared by regioselective periodate oxidation of hydroxyl groups of cellulose at C2 and C3 of pyranose cycle.[9,10] Structure of DAC and simplified reaction scheme between DAC and PVA is given in Figure 1. Raw DAC is insoluble in aqueous media and must be solubilized by hot water prior to its utilization in solution-based processes.[11] DAC features two highly reactive aldehyde groups per each

oxidized unit, which can be used for crosslinking of polymers bearing hydroxyl side groups (Figure 1). However, DAC was deemed to be rather unstable in solution.[12] The presumed need to prepare a fresh crosslinker for every use reduced its potential in practical applications.[13] Only recently, we have shown that the stabilization of an aldehyde group content over a prolonged period can be achieved by decreasing the pH of the solution to 3.5.[10]

DAC has several advantages over currently used organic crosslinkers such as glutaraldehyde (GA). Firstly, DAC can be prepared using cellulose from renewable resources [14] and consumed periodate salt can be easily regenerated and re-used making the whole process sustainable.[15] Secondly, DAC is considerably less toxic than GA, [16] which is particularly important to the preparation of biomaterials for medical and cosmetic sector. Last but not least, DAC is more effective crosslinker than GA at the same concentration of aldehyde groups. [17] This is a result of "two-phase" network topology found in DAC hydrogels. [16–18] Briefly, while small GA molecules are uniformly distributed through the hydrogel network, the much larger DAC macromolecules can crosslink numerous PVA chains simultaneously, thus creating regions with very high crosslink density, which are embedded in PVA matrix. Resulting PVA/DAC hydrogels thus have better mechanical properties than PVA/GA counterparts.[18]

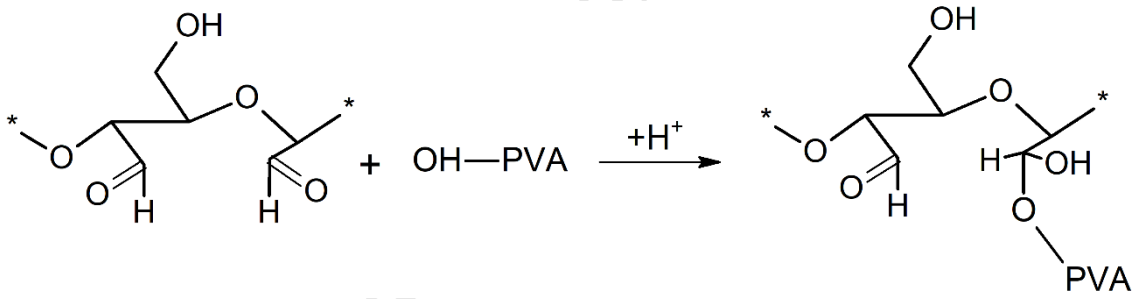

Figure 1 The structure of DAC and a simplified reaction scheme between –CHO and –OH groups of 2,3-dialdehyde cellulose and PVA in an acidic environment, respectively.

Here, DAC is used as a crosslinker for preparation of thin hydrogel films optimized for transdermal drug delivery, wound dressings and cosmetic products. The role of varied amount of crosslinker and different weight-average molecular weight (M_w) of PVA to the network parameters, porosity, viscoelastic properties, cytotoxicity and biocompatibility of prepared thin films is discussed together with release kinetics and transdermal absorption of two model drugs, rutin and caffeine.

Rutin is the glycoside composed of quercetin and rutinose (α-L-rhamnopyranosyl-(1→6)-β-D-glucopyranose). It is a flavonoid found in a wide variety of plants including buckwheat, tea and citrus fruit. It is highly versatile in its biological activity because it exhibits antioxidative, cytoprotective, vasoprotective, anticarcinogenic, neuroprotective and cardioprotective properties.[19] It finds numerous applications in cosmetics, because it stabilizes the vascular walls, prevents them from cracking and counteracts the manifestation of dilated veins. It is

also utilized in wound dressing and healing applications because it shows anti-microbial and anti-inflammatory activity and reduces oxidative stress in the wounded area.[20,21]

Caffeine is a stimulant of the central nervous system and is often used as a model drug for studying the penetration of hydrophilic substances across the skin barrier.[22,23] Caffeine-saturated hydrogels can stimulate the nervous system, support lymphatic system, prevent excessive fat accumulation in the skin and help protect the skin from photodamage.[22,23]

2. EXPERIMENTAL

2.1 Materials

Two types of poly(vinyl alcohol) (PVA) with 88% degree of hydrolysis with different M_w (130 and 31 kDa, respectively) were used (Sigma Aldrich Co.). Alpha cellulose (M_w = 109 kDa)[24] (Sigma Aldrich Co.), sodium periodate ($NaIO_4$) (Penta, Czech Republic), ethylene glycol, hydrochloric acid (HCl) (Penta, Czech Republic) were employed in the synthesis of 2,3-dialdehydecellulose (DAC) and in the subsequent preparation of hydrogels. The prepared PVA/DAC hydrogels were saturated with rutin and caffeine (Sigma Aldrich Co.). The mouse embryonic fibroblast cell line (NIH/3T3, ECACC) was used for the determination of biological properties. DMEM (Biosera, France) containing 10 % of calf serum (Biosera, France) and 100 U/mL Penicillin/Streptomycin (Biosera, France) was used as a culture media. Cells were incubated at 37 °C in a 5% CO_2 humid atmosphere. Phosphate buffer saline (PBS) (Invitrogen, USA) was used for cells washing. Cells were cultured on Techno plastic (TPP, Switzerland), using Tetrazolium kit (MTT cell proliferation assay, Duchefa Biochemistry, The Netherlands). The other chemicals used in biological testing include formaldehyde (Penta, Czech Republic), Triton X (Sigma Aldrich Co.), Hoechst 33258 (Invitrogen, USA) and ActinRed™ 555 (Thermo Fisher Scientific, USA. For transdermal testing gentamicin sulfate (HiMedia Laboratories), formic acid (HCOOH), and methanol (Penta, Czech Republic) were used. All chemicals were of analytical purity and were used as received without further purification. Demineralized water was used throughout the experiments.

2.2 Preparation of crosslinked PVA/DAC hydrogels

In the first step, the 2,3-dialdehydecellulose (DAC) was prepared by oxidation of alpha cellulose by $NaIO_4$ using a 1:1.2 molar ratio of reactants (DAC : periodate) following earlier works.[10,17,18,25] Briefly, to achieve high conversion of cellulose to DAC, 10 g of cellulose was suspended in 250 mL of water containing 16.5 g of sodium periodate. The mixture was then stirred in the dark for 72 h at 30 °C. The oxidation was stopped by addition of 10 mL of ethylene glycol and the product washed and filtered. Resulting raw DAC was suspended in 175 mL of water and solubilized at 80 °C for 7 h.[11] Next, the solubilized DAC was cooled, centrifuged (10 min, 10 000 RPM) and the solution was transferred to a 200 mL volumetric flask. The weight concentration of solubilized DAC was determined (42.3 ± 1.3 mg/mL) by simple weight analysis (i.e. solution evaporation and residue weighing). The prepared DAC solution of known concentration served for crosslinking of PVA.

In the second step, 10 g of each PVA type (M_w 31 000 or 130 000 g/mol) was dissolved in 80 mL of water at 90 °C. Subsequently, the catalyst (10 mL of 1.3 M HCl) and defined amount

of DAC corresponding to 0.25 wt.% and 1 wt.% (with respect to the weight of PVA) was added. The prepared reaction mixtures were thoroughly stirred and poured onto Petri dishes (*d* = 140 mm) and left to dry at 30 °C until constant weight. The crosslinking reaction between PVA and DAC occurs during the drying of the reaction mixture, where dehydration of –CHO groups of DAC causes the formation of hemiacetals with hydroxyl groups of PVA. Simplified reaction scheme between –CHO of DAC and –OH group of PVA in an acidic environment is shown in Figure 1.

The prepared thin films were then thoroughly washed in water to remove uncrosslinked material, and disc-shaped samples of 15 and 50 mm in diameter were cut out and stored in aseptic medium (70% ethanol solution) until used. A small part of the PVA/DAC samples was left unwashed for determination of network parameters (gel fraction). Designation and composition of the prepared PVA/DAC samples are listed in Table 1.

Table 1 Designation of PVA/DAC samples, their composition and M_w of the PVA used.

Sample	**PVA (g)**	**M_w PVA (kDa)**	**DAC (wt.%)**	**DAC (g)**
L-31	10	31	0.25	0.025
H-31	10	31	1	0.1
L-130	10	130	0.25	0.025
H-130	10	130	1	0.1

The estimation of network parameters, measurement of viscoelastic properties, BET and SEM analysis, drug release kinetics, cytotoxicity and transdermal absorption of prepared hydrogels were subsequently investigated.

2.3 Network parameters

The network parameters were estimated based on the measurements of swelling and weight change of prepared 15 mm disc-shaped PVA/DAC xerogel samples (6 specimens for each). Unwashed discs were weighed and then thoroughly washed for one week with regular changing of water. Subsequently, the swollen discs were gently dried to remove excess water, weighed and dried at 30 °C till constant weight. The network parameters were determined using equilibrium swelling theory suggested by Flory and Rehner.[26] The constants used for the calculation of network parameters include the specific volume of PVA polymer v = 0.788 cm^3/g, the PVA density ρ_p = 1.27 g/cm^3, the molar volume of water (V_1) at 25 °C = 18.069 cm^3/mol, the polymer-solvent interaction parameter (χ_1) = 0.464, the average bond length l = 1.54 Å, the characteristic ratio of PVA chain C_n = 8.9 and the molecular weight of PVA unit M_r = 44 g/mol. Following equations were used to calculate network parameters.[27],[10]

Equilibrium swelling [%] was obtained according to Eq. 1, where M_E is the mass of the hydrogel swollen to the equilibrium state, and M_0 is the mass of the washed and dried hydrogel.[28]

$$\text{Equilibrium swelling (\%)} = \frac{M_E - M_0}{M_0} \times 100 \quad (1)$$

Equilibrium water content (*EWC*) describes the maximum amount of water absorbed by the hydrogel. M_s is the mass of the sample swelled under equilibrium conditions, and M_0 is the mass of the washed and dried hydrogel.[29]

$$EWC\ (\%) = \frac{M_s - M_0}{M_s} \times 100 \tag{2}$$

The gel fraction was calculated using Eq. (3), where M_0 is the weight of the dried hydrogel after extraction of the soluble fraction in the hydrogel and M_{int} is the weight of the dry and non-washed hydrogel.[28]

$$\text{Gel fraction } (\%) = \frac{M_0}{M_{int}} \times 100 \tag{3}$$

The average molecular weight between crosslinks (M_c), where M_n is the average number molecular weight of the initial uncrosslinked polymer, v is the specific polymer volume, V_1 is the molar volume of water, $V_{2,s}$ is the polymer volume fraction and χ_1 is the polymer-solvent interaction parameter.[26]

$$M_c\ (\text{g/mol}) = \frac{M_n}{2} - \frac{\left[(V_{2,s})^{\frac{1}{3}} - \frac{V_{2,s}}{2}\right]}{\left(\frac{v}{V_1}\right)\left[\ln(1-V_{2,s}) + V_{2,s} + \chi 1 (V_{2,s})^2\right]} \tag{4}$$

Polymer fraction ($V_{2,s}$), where M_s/M_0 is the weight ratio of dry to swollen hydrogel at equilibrium, ρ_p is the density of the polymer and ρ_w is the density of water.[30]

$$V_{2,s} = \left[1 + \frac{\rho_p}{\rho_w}\left(\frac{M_s}{M_0} - 1\right)\right]^{-1} \tag{5}$$

Calculation of the crosslink density (ρ_c). [26],[31]

$$\rho_c\ (\text{mol/cm}^3) = \frac{1}{v M_c} \tag{6}$$

The mesh size (ξ):

$$\xi\ (\text{Å}) = V_{2,s}^{-1/3} (??_0^{\ 2})^{1/2} \tag{7}$$

Where $(??_0^{\ 2})^{1/2}$ is the end-to-end distance of the unperturbed (solvent-free) state.

$$(??_0^{\ 2})^{1/2} = l \left(\frac{2 \times M_c}{M_r}\right)^{1/2} \times C_n^{\ 3/2} \tag{8}$$

2.4 Measurement of viscoelastic properties

Disc samples (d = 15 mm, 6 specimens per sample) were measured in an equilibrium swollen state using a rotational rheometer Anton Paar MCR 502 (Anton Paar, Austria) equipped with D-PP15 shaft using a roughened aluminium plate with 15 mm diameter and ground plate with glued sandpaper both used to prevent slipping of samples during measurement. The measurement was performed at laboratory temperature in oscillation mode in frequency sweep from 1 to 10 Hz by applying a constant strain of 1 %.

2.5 BET and SEM analysis

Lyophilized PVA/DAC cryogels were initially degassed at 75 °C for 24 h. Specific surface area (α_{BET}), total pore volume (V_p) and mean pore diameter of cryogels was determined by multipoint Brunauer-Emmet-Teller (BET) analysis of adsorption isotherms recorded at 77 K utilizing high precision surface area analyzer Belsorp-mini II (BEL Japan Inc., Japan). The measurement was carried out in triplicates. These materials were also analyzed by scanning electron microscopy (SEM) employing Nova NanoSEM 450 microscope (FEI, Czech Republic) operated at 5 kV accelerating voltage. Ahead of SEM imaging, cryogels were sputtered with gold-palladium nanoparticles to suppress the charge accumulation effect.

2.6 Loading and release

H-31, L-130 and H-130 samples of approximately 500 mg and 15 mm in diameter were loaded by biologically active compound by submerging into a 50 mL of stock solution of 0.1 mg/mL (rutin) or 10 mg/mL (caffeine) and shaken for 72 h at 37 °C. Loaded samples were then used to study the drug release kinetics. For this purpose, three samples from each hydrogel were placed in separate closed containers containing 10 mL of demineralized water and shaken at 37 °C in the dark. Aliquots of 1 mL were collected in given times over 96 h and analyzed using UV-VIS spectrometer Perkin Elmer Lambda 1050 (Perkin Elmer Inc., USA) using characteristic peaks at 353 nm (rutin) and 273 nm (caffeine). The experiments were performed in triplicates.

2.7 Cytocompatibility of hydrogels

The cytocompatibility tests included 1) evaluation of cytotoxicity of hydrogel extracts and 2) cell growth in the presence of hydrogel and in direct contact with their surfaces. The cytotoxicity was tested according to ISO 10 993-5. All tests were performed in quadruplicates.

1) Extracts from L-130, H-130 and H-31 specimens were prepared according to ISO 10993-12 in the concentration of 0.1 g of swollen gels per 1 mL of culture media. The tested samples were extracted in culture medium for 24 hours at 37 °C under constant shaking. The parent extracts (100%) were then diluted in culture medium to obtain a series of dilutions with concentrations of 75, 50, 25, 10, and 1 %. The mouse embryonic fibroblast (NIH/3T3) cells were seeded into 96 well plates in concentration 10^5 cells per mL and placed to the incubator for pre-cultivation for 24 hours at 37 °C. After the pre-incubation period, the extracts were added and cells incubated for another 24 h. Determination of cell viability after exposure time was performed by MTT assay. The reference wavelength was set to 570 and 690 nm, respectively. The results are presented as the relative cell viability compared to the reference (cells cultivated on tissue plastic only in culture medium), where reference corresponds to 1 (100% cell viability).

2) For the test of cell growth in the presence of hydrogels, cells were seeded on culture plastic plates in concentration 10^5 cells per mL and pre-incubated till they reached sub-confluence. The hydrogels were placed in the centre over the adherent cells. Cells were checked every day by an inverted phase-contrast microscope Olympus IX 81 (Olympus, Japan) until the

reference reached full confluency (96 h). Cell viability was measured by MTT assay in the same conditions as in the cytotoxicity of hydrogel extracts after 48 and 96 h.

For the determination of cell adherence and growth on the surface of hydrogels, cells were seeded directly on the samples surfaces in concentration 5×10^4 cells per cm^2. After 48 h samples were fixed with 4% formaldehyde for 15 minutes, washed with PBS, permeabilized with 0.5% Triton X for 5 minutes and subsequently stained with Hoechst 33258 and ActinRed^{TM} 555 for 30 minutes in the dark. Cells were observed using an inverted fluorescence phase-contrast microscope Olympus IX 81 (Olympus, Japan).

2.8 Transdermal absorption tests in vitro

Tests were conducted according to the OECD Test Guideline for Skin Absorption: *In vitro* method, using the skin from pig ear. The pig's ear lobe was shaved and the inner part of the auricle was separated from the underlying cartilage. Square skin samples of 3×3 cm were cut out from the separated skin. The skin samples were then placed in test cells and their skin integrity was determined using a UNI-T UT71D multimeter. Samples with a resistance below 5 mΩ were excluded.

Disc-shaped samples of individual hydrogels were added to the prepared skin samples. Prior to insertion, the hydrogels were loaded with caffeine by shaking for 120 h at 37 °C in 10 mg/mL caffeine. Testing was performed on an automated diffusion cell system with the continuous flow of receptor liquid through samples Fraction Collector FC33 (Permegear, USA). All experiments were performed in triplicates. The receptor fluid (PBS buffer and 0.05% gentamicin sulfate) was collected for 24 h at a constant flow rate of 2 mL/h. After completion of the measurements, the fractions obtained at pre-set times (1–24 h) were stored at -20 °C until analysis. The individual samples were then filtered and analyzed by liquid chromatography employing HPLC chromatograph Breeze 1525 with UV-VIS detector (Waters Corporation, USA). Chromatographic separation of the caffeine within the samples was carried out isocratically on a Kinetex C18 100A column (150×4.6 mm, 2.6 µm) (Phenomenex, USA). The mobile phase consisted of 0.2% HCOOH and methanol in a 75/25 ratio, the temperature was set to 30 °C, the flow rate 0.7 mL/min. The wavelength used for detection was 272 nm.

3. RESULTS AND DISCUSSION

Four types of hydrogel samples differing in concentrations of DAC and M_w of PVA were prepared, see Table 1. Only the network parameters were determined for the sample L-31 (L stands for lower amount of the DAC, 0.25 wt.%, number 31 is the molecular weight of PVA in kDa, cf. Table 1). The reason being its poor physical properties caused by combination of low crosslinker concentration and low M_w of PVA. Sample L-31 teared and disintegrated even during gentle manipulation, which prevented meaningful characterization as some techniques would be influenced by macroscopic faults in hydrogel structure, making obtained data unreliable. Other three types of hydrogel samples (L-130, H-31 and H-130, H stands for higher concentration of crosslinker – 1 wt.%, number 130 is the molecular weight of PVA in kDa, cf. Table 1) were characterized by full set of methods described above.

3.1 Network parameters

Based on the equations given in Section *2.3*, the network parameters of all types of PVA/DAC hydrogel samples (L-130, H-130, L-31, H-31) were determined, Table 2. Unsurprisingly, the swelling of hydrogel matrices and *EWC* depends on both the amount of DAC and the M_w of PVA. The lower the amount of crosslinker and the lower the M_w of PVA, the more the hydrogel swells. Thus, sample L-31 has the largest swelling, equal to almost 80-times of its dry mass. On the other side, sample H-130 swells only about 3.5-times. Conversely, the gel fraction increases with increasing amounts of DAC and M_w PVA, thereby sample H-130 shows the largest gel fraction and sample L-31 the smallest one.

The dependence of average molecular weight between crosslinks (M_c), crosslink density (ρ_c), and mesh size (ξ) on both observed factors is, however, not so straightforward. As one may expect, decreasing the amount of DAC results in higher separation of crosslinked regions (higher M_c), which reduces ρ_c and increase the ξ of respective samples. However, the influence of M_w of PVA on M_c and ρ_c actually differs for different the amounts of crosslinker. Increased M_w of PVA is causing a significant decrease of M_c (an increase of ρ_c) in H-series (1 % of DAC), but the opposite trend was found in L-series (0.25 % of DAC). Notably, the ξ is smaller for PVA with M_w = 130 kDa in both series.

Table 2 Network parameters (the equilibrium swelling, the equilibrium water content *EWC*, the gel fraction, the average molecular weight between crosslinks M_c, the crosslink density ρ_c and the mesh size ξ) calculated for the prepared hydrogel samples. Data represent average of six measurements with standard deviations.

Sample	**Equilibrium swelling (%)**	***EWC* (%)**	**Gel fraction (%)**	M_c **(g/mol)**	ρ_c **(μmol/cm^3)**	ξ **(Å)**
L-31	7900 ± 800	98.7 ± 0.1	12 ± 0.8	12380 ± 20	103 ± 1	508 ± 17
H-31	710 ± 20	87.6 ± 0.3	47.7 ± 0.9	6410 ± 160	198 ± 5	169 ± 4
L-130	1150 ± 90	92 ± 0.6	58.8 ± 1.8	20660 ± 1880	62 ± 6	352 ± 25
H-130	350 ± 10	77.8 ± 0.3	88.8 ± 0.2	2890 ± 90	440 ± 14	93 ± 2

The variation of M_c and ρ_c between series is likely related to the nature of PVA/DAC network, which is composed of two types of interactions – the PVA/DAC chemical crosslinks complemented by residual physical interactions (hydrogen bridge network and chain entanglements) between the PVA macromolecules.[17] It is reasonable to assume that chemical crosslinking is more pronounced in H series hydrogels, particularly in for H-130 sample where longer PVA chains offer considerably more crosslinking hot-spots. Thus, the sample H-130 exhibits the smallest M_c and ξ and the highest ρ_c of all. In more sparsely crosslinked L series, the effect of residual physical crosslinking of longer PVA (130 kDa)

chains provides additional stabilization to the hydrogel network. Hence, despite L-130 sample having the lowest-density network with highest M_c and lowest ρ_c from all samples, its ξ is lower than in case of L-31, and its physical properties are sufficient for easy handling in contrast to sample L-31, which had to be excluded from further analyses.

To summarize, although the role of the amount of the crosslinker governs the network parameters of hydrogels (i.e. four-times less of DAC results in up to 10-times the swelling in L-31 vs. H-31), it is further accentuated by changing the M_w of PVA, which influences the hydrogel network mainly at the (macro)molecular level.

3.2 Analysis of viscoelastic properties

Oscillatory shear rheometry utilizing frequency sweep from 1 Hz to 10 Hz and constant strain of 1 % was used to study the viscoelastic properties of prepared hydrogels. The dependence of storage modulus ($G^{'}$) and loss modulus ($G^{''}$) on angular frequency is given in Figure 2A. The $G^{'}$ values of PVA/DAC hydrogel samples range from more than 2100 Pa for sample H-130 to about 150 Pa for sample L-130. The $G^{''}$ values range from about 190 Pa for sample H-130 to about 4.3 Pa for sample L-130. As expected, [18] the results follow the trend of ρ_c (see Table 2), because the denser mesh have a higher elasticity than the sparser one, which will, in turn, have more viscous-like behavior. Hence, the lowest $G^{'}$ and $G^{''}$ values were observed for the L-130 sample with the lowest crosslink density. The effect of the M_w of PVA is observable for H series hydrogels, where four-times lower M_w of PVA results in decrease of both $G^{'}$ and $G^{''}$ by approx. 75%.

Analogous correlations between the amount of crosslinker and the M_w of PVA were found for the complex dynamic modulus (G^*) and the damping factor ($tan\ \delta$). The complex modulus G^* was calculated as the square root of the sum of the square of storage and loss moduli in the selected range of oscillatory measurement at ambient temperature, Figure 2C. The range of G^* values is from more than ~2200 Pa for H-130 to ~150 Pa for sample L-130. The $tan\ \delta$ is defined as the ratio between loss and storage modulus ($G^{''}/G^{'}$) and gives a measure of viscous to elastic component of the material. The damping factor ranges from 0.09 for sample H-130 (most elastic) to 0.03 for sample L-130 (the most viscous), Figure 2D.

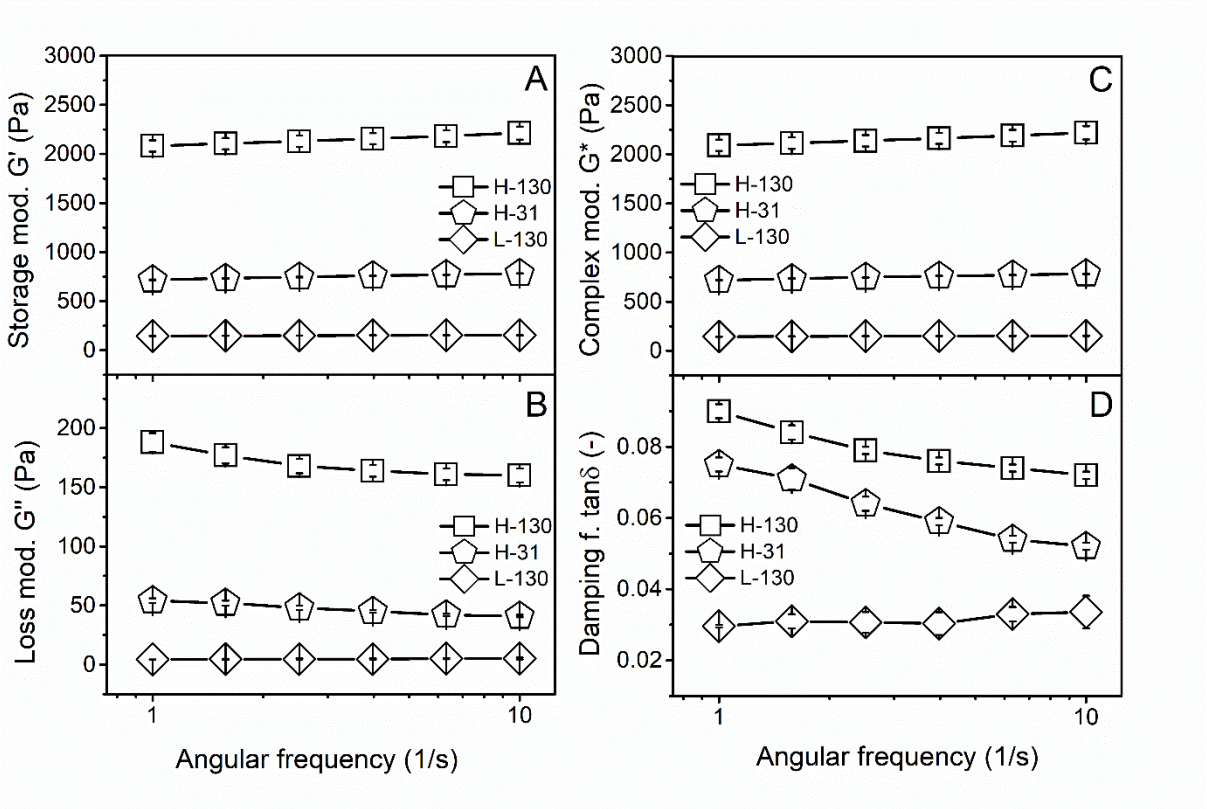

Figure 2 Dependence of the storage modulus ($G^{'}$) and the loss modulus ($G^{''}$) of PVA/DAC hydrogel samples on the angular frequency (part A and B), dependence of the calculated complex modulus (G^{*}, part C) and the damping factor (*tanδ*, part D) on the angular frequency. Measurements were repeated six times; error bars express standard deviations.

To summarize, the most viscous and the least elastic material is the least crosslinked sample L-130. The most elastic is sample H-130. Notably, viscoelastic properties of sample H-31 are generally closer to L-130 than to H-130 despite being prepared by using the same amount of crosslinker as the latter. This demonstrates a considerable influence of the PVA matrix on the rheological properties of the hydrogels.

3.3 BET and SEM analysis

Samples of PVA/DAC hydrogels were lyophilized, and their specific surface area (α_{BET}), total pore volume (V_p), mean pore diameter and adsorbed volume of nitrogen (V_a) measured, see Figure 3. The α_{BET} value for sample L-130 (31.1 ± 0.9 m^2/g) is of the order of magnitude higher than the values for samples H-130 (2.0 ± 0.1 m^2/g) and H-31 (2.2 ± 0.1 m^2/g). Furthermore, the total pore volume (V_p) exhibits the same trend as α_{BET}, it is about ten times higher for L-130 (0.218 ± 0.007 cm^3/g) than in H-series hydrogels (H-130 = 0.021 ± 0.001 cm^3/g and H-31 = 0.031 ± 0.002 cm^3/g, see Figure 3C). This difference is closely related to the extent of cavitation induced by the lyophilization and indirectly linked to the water absorption capability of the hydrogel. Interestingly, mean pore diameter do not follow described trend. Largest pore diameter was observed for H-31 sample (54.6 ± 3.3 nm), followed by H-130 sample (41.5 ± 2.1 nm) and L-130 sample (28.1 ± 0.8 nm). The H-series

cryogels thus have fewer larger pores, while L-130 contains a larger number of smaller pores in its structure.

Cryogel samples were further analyzed by scanning electron microscopy (SEM). In agreement with α_{BET} values, surface of L-130 hydrogel sample was found to be highly porous, see Figure 3D, while the H-31 sample showed slightly larger surface pores than the H-130 sample, but the difference is not very significant.

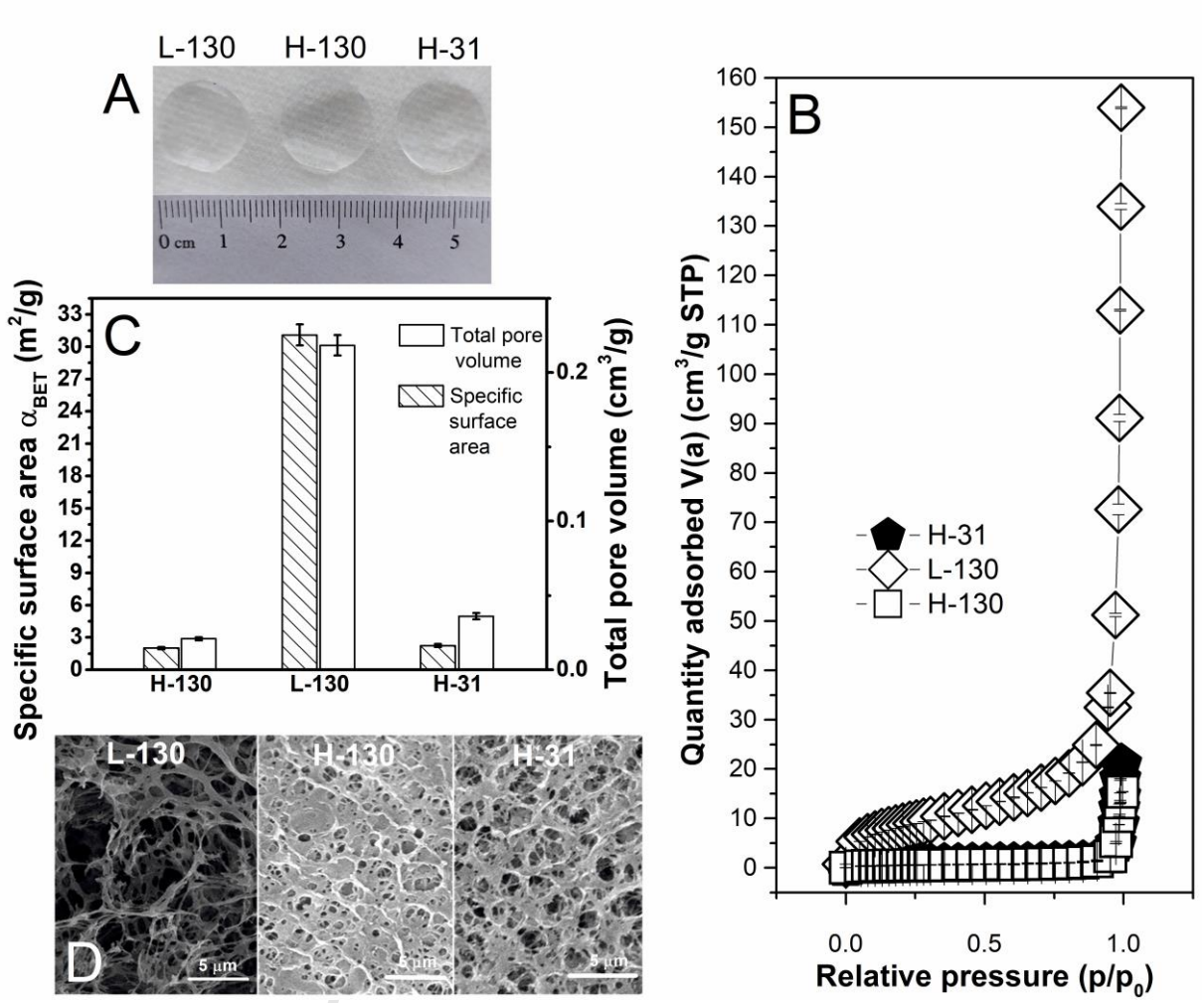

Figure 3 Photographs of swollen hydrogel samples (part A), dependence of quantity of the adsorbed volume of nitrogen per cryogels mass (V_a) on the relative pressure p/p_0 (part B), the specific surface area α_{BET} and total pore volume (V_p) of prepared PVA/DAC cryogels (part C), and micrographs of individual PVA/DAC samples taken with SEM at 30.000x magnification (part D). Measurements were performed in triplicates; error bars represent standard deviations.

To summarize, while both α_{BET}, V_p and V_a increase significantly with the decreasing amount of DAC, the M_w of PVA seems to influence the mean pore size. It should be noted that combination of the low amount of DAC and high-molecular-weight PVA allowed preparing

highly porous materials with mechanical properties allowing reasonable handling, which was not possible by using PVA with lower molecular weight (sample L-31).

3.4 Loading and release study

Samples of individual hydrogels were loaded with rutin or caffeine, see Section *2.6* for more details. The loaded hydrogel samples were subsequently put into separate containers containing 10 mL of water and release of rutin (Figure 4A) and caffeine (Figure 4B) evaluated by UV-VIS spectroscopy.

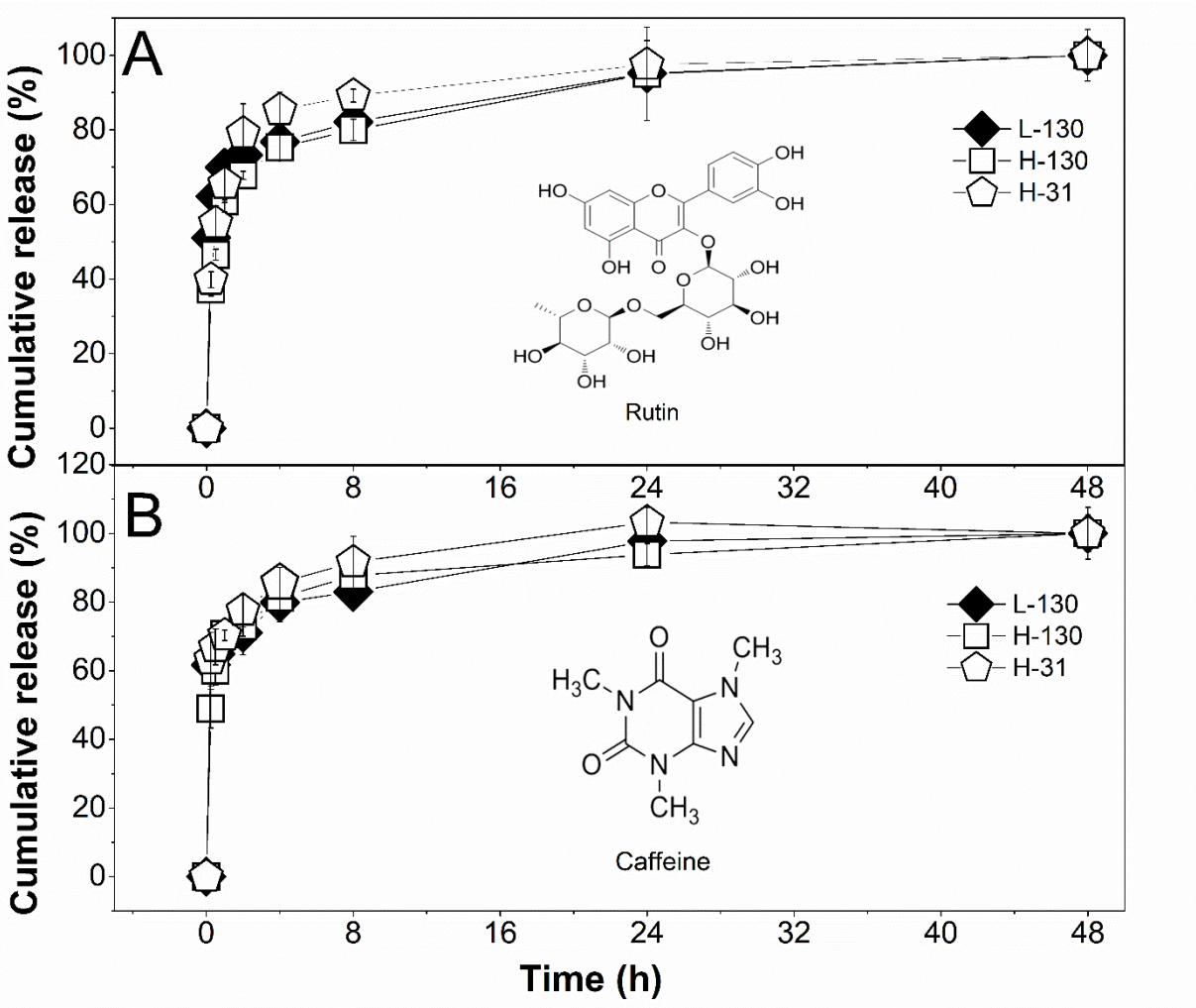

Figure 4: Cumulative release of rutin (part A) and caffeine (part B) from L-130, H-31 and L-130 hydrogel samples. All experiments were performed in triplicates; error bars represent standard deviations.

Release rates of relatively small caffeine molecules (M = 194 g/mol, Figure 4B) from all three tested materials are identical within the experimental error. The effect of the network parameters is only observable for larger rutin (610 g/mol), where fastest release after 8 h was observed for H-31 sample, while both 130-series samples showed nearly identical release kinetics. This might be related to lower M_w of PVA influencing the pore size (see previous

section), but the difference is relatively minor and more tests would be needed to confirm this observation.

Small differences in burst release kinetics are most likely caused by low thickness of prepared hydrogel films. Because most of the drug is situated in the vicinity of the thin film surface, the diffusion path is very short, which together with hydrogel mesh size being significantly larger than the diameter of studied molecules (100–350 Å, Table 2), minimizes the impact of hydrogel network to the drug release rate. This may be improved by employing thicker films or by modification of drug loading procedure.

Nevertheless, the observed burst release kinetics with up to 80–90 % of compounds released in 8 h, is considered to be suitable for intended topical drug delivery applications, where expected time of application is in order of hours rather than days.

3.5 Biological testing

Biological evaluation included (i) determination of cytotoxicity of hydrogel extracts in culture media prepared according to ISO 10993-12 and (ii) observation of cell growth and morphology in the presence of hydrogels as well as directly on the gel surface. Cytotoxicity of hydrogel extracts was evaluated using mouse embryonic fibroblast cell line (NIH/3T3) according to ISO 10 993-5, see Figure 5.

The amount of DAC did not have any observable impact to the cytotoxicity of hydrogel extracts and all materials can be considered non-toxic according to ISO 10 933-5.

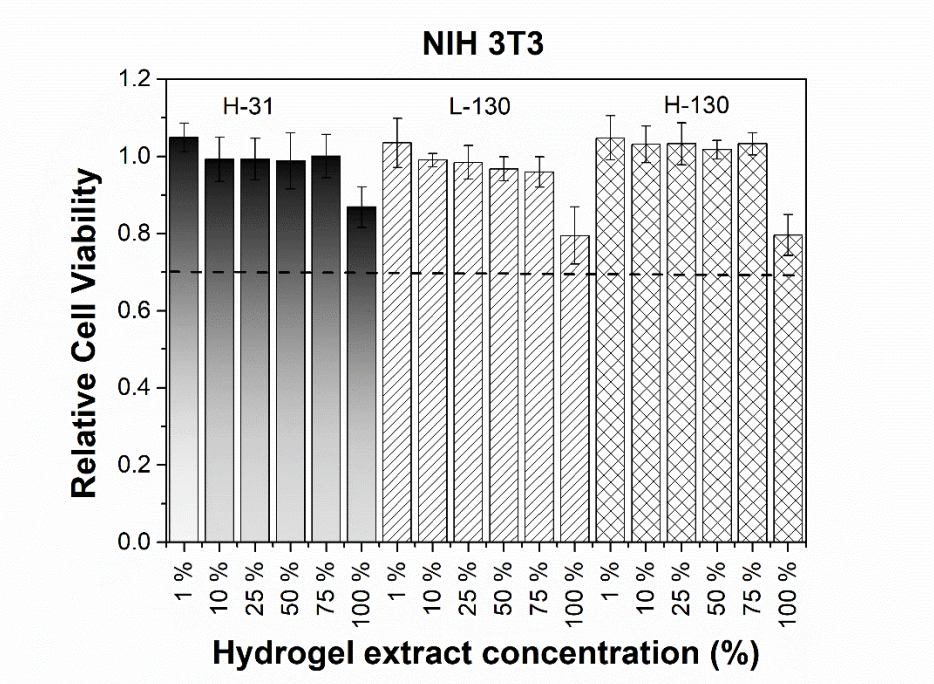

Figure 5 Relative cell viability of cells incubated with PVA/DAC hydrogel extracts of different concentrations (1–100%) tested on mouse embryonic fibroblast cell line (NIH/3T3). Measurements were performed in quadruplicates; error bars represent standard deviations.

Subsequently, the cell growth and morphology in the presence of hydrogels was studied for 96 h. Cell viability was quantified by MTT assay, and qualitative analysis was done by observation under the microscope. Cell morphology was checked every day until reference reached confluency. Results are shown in Figure 6, together with micrographs of cells cultivated in the presence of hydrogels for 96 h.

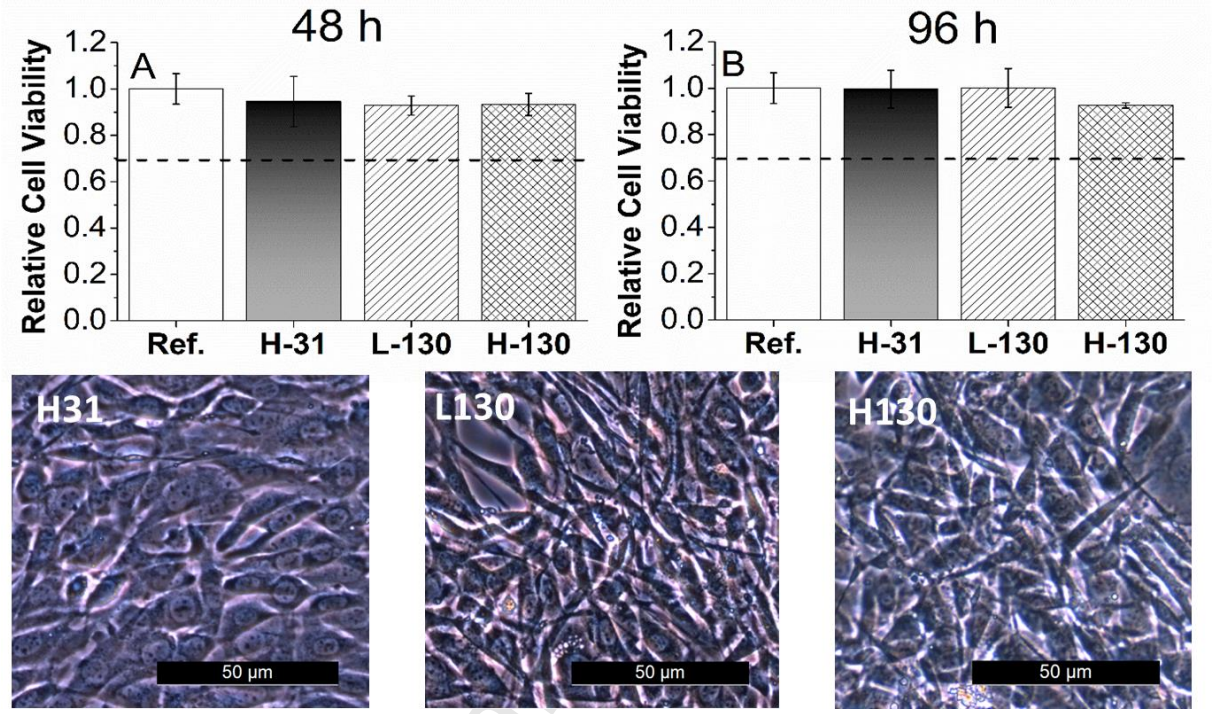

Figure 6: Relative NIH/3T3 cell viability of cells incubated in the presence of hydrogel samples for 48 and 96h, respectively, and micrographs of cells incubated for 96 h. Experiments were performed in quadruplicates; error bars represent standard deviations.

The presence of hydrogel samples has no observable effect on cell growth or morphology. Cells were growing at the same rate in the presence of hydrogels as on the culture plastic and reached full confluency at the same time (Figure 6, top). Likewise, the morphology was not affected by the hydrogels in any way, and fibroblasts retained their typical elongated shapes, see micrographs in Figure 6. Cells were also seeded directly to the hydrogel surface in an attempt to observe they growth and morphology in direct contact with the hydrogel. However, cells did not adhere to hydrogel surface at all, making the evaluation impossible.

It should be also noted that no degradation of hydrogels was observed during the tests or when samples were kept under *in vitro* conditions (submerged to culture medium, seeded with NIH/3T3 cells, 37°C) for one week. Surface of samples remained smooth, without signs of weathering or degradation and no difference in weight of the samples before and after the tests was observed.

To summarize, absence of cell migration/attachment to the hydrogel surface, no observable impact of hydrogel presence on the cell growth together with no observable degradation

supports the suitability of hydrogel films as wound dressings. Additional tests are however required before biosafety *in vivo* can be claimed.

3.6 Transdermal absorption study

Transdermal absorption was studied using caffeine-loaded hydrogel samples. Caffeine was selected as a model substance for the study of transdermal absorption of hydrophilic compounds.[22] Hydrogel samples (1 cm in diameter) were loaded with caffeine and transdermal absorption of caffeine studied using skin from pig's earlobe, see Section *2.8* for more details. Amount of absorbed caffeine was determined by HPLC analysis.

The total amount of caffeine in the samples and calculated dose per 1 cm^2 skin is given in Table 4. All samples were loaded by the same method, but the total dose of caffeine differs between samples because of their different EWC, gel fractions and equilibrium swelling. The highest amount of caffeine was loaded in the sample L-130 (~900 µg), while sample H-130 was able to absorb the smallest amount (~500 µg). The aqueous caffeine solution containing a total dose of 250 µg was used as a reference.[23]

Table 4 The amount of caffeine in the samples (µg) and the dose of caffeine per cm^2 of skin.

Sample	**Total dose of caffeine (µg)**	**Dose per cm^2 (µg/cm^2)**
L-130	896 ± 8	1134 ± 10
H-31	660 ± 6	832 ± 7
H-130	495 ± 1	625 ± 1
Reference	250	320

The total amount of transdermally absorbed caffeine [ng] is shown in Figure 7A, the time profile of caffeine absorption [ng/mL] in Figure 7B, total amount of transdermally absorbed caffeine relative to applied dose [%] in Figure 7C and the time profile of caffeine absorption relative to applied dose [%] in Figure 7D. Results show that caffeine penetrates the skin relatively slowly over the entire monitored time interval (24 h). According to Trauer *et al.*,[23] this is a result of the absence of blood supply to the skin during the *in vitro* study because much faster absorption of caffeine through the skin of a living organism was observed. As a result, only between 0.07 % and 0.2 % of total caffeine dose crosses the skin barrier within 24 h under the employed setup (Figure 7C and 7D), which can be explained by caffeine hydrophilicity making its penetration through *stratum corneum* challenging.[32] This is in agreement with findings of other authors, including Trauer *et al.*,[23] Bonina *et al.*[33], Santander-Ortega *et al.*[34] and Pilloni *et al.*[35] who also observed the transdermal caffeine absorption in the order of tenths of the percent of the applied dose using a variety of different carriers.

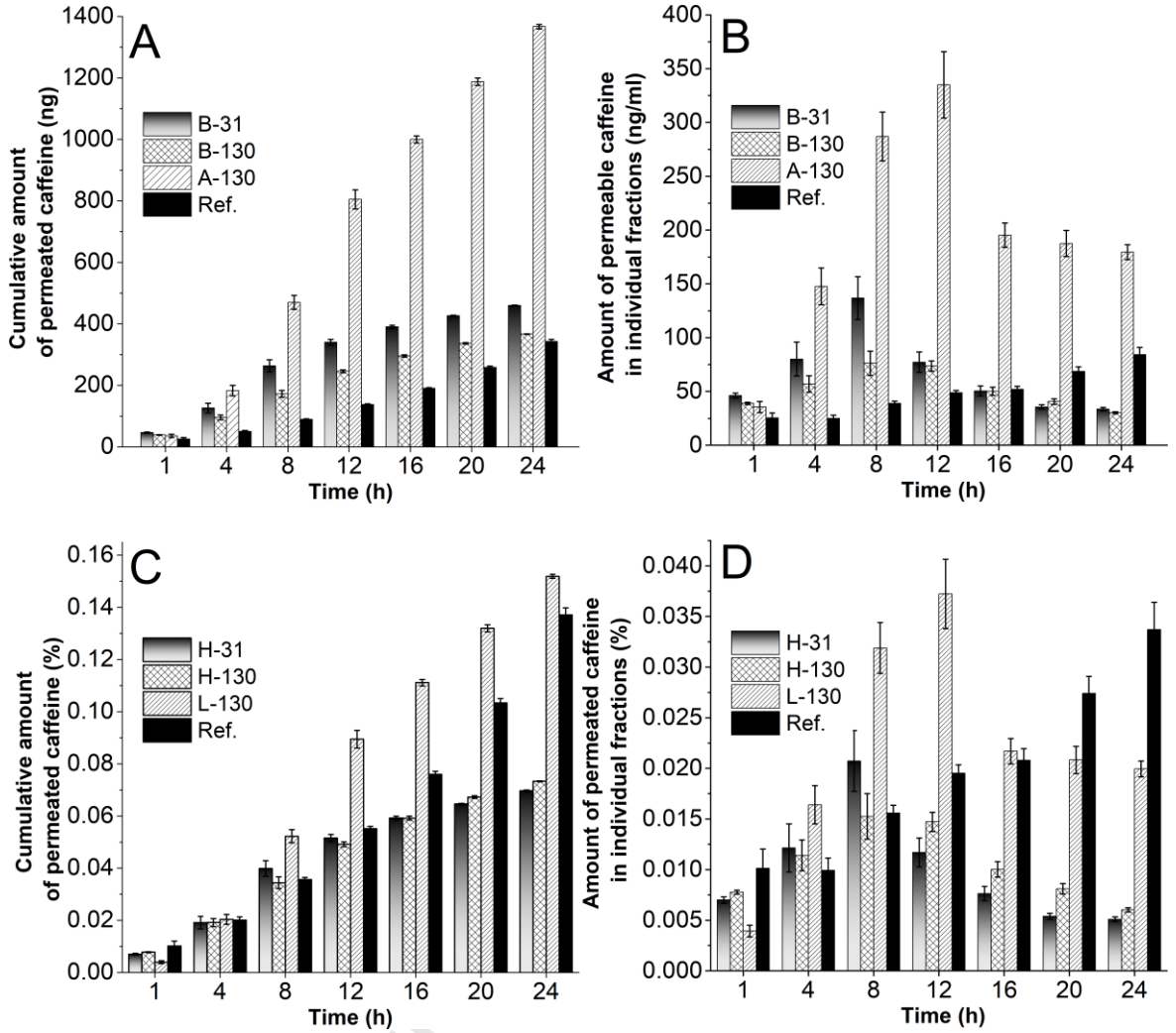

Figure 7 The cumulative amount of permeated caffeine [ng] (part A), the time-dependent amount of permeated caffeine [ng/mL] (part B), total amount of transdermally absorbed caffeine relative to applied dose [%] (part C) and the time profile of caffeine absorption relative to applied dose [%] (part D). Ref. stands for the reference caffeine solution. Measurements were performed in triplicates; error bars represent standard deviations.

Despite the relatively low amount of transdermally absorbed caffeine, differences between the samples are clearly visible. The highest total amount of absorbed caffeine (1400 ng/0.15%) was observed for the L-130 sample, while only between 350–450 ng (0.06-0.07%) of caffeine was absorbed from H-series samples over 24 h. This corresponds to the average caffeine penetration of 72.1 ng.cm^2/h for L-130, 24.3 ng.cm^2/h for H-31, 19.3 ng.cm^2/h for H-130 and 18.1 ng.cm^2/h for caffeine solution. On the other hand, when the differences in applied dose are considered (Figure 7C), only the sample L-130 overcomes the reference solution in terms total caffeine absorption with respect to applied dose. However, while the amount of the drug absorbed from caffeine solution linearly increases with time, the amount of caffeine absorbed

from the hydrogels peaks between 8 - 12 h, respectively (Figure 7B and 7D) showing higher effectivity of initial caffeine absorption from hydrogels.

Comparing individual hydrogel samples, higher effectivity of caffeine absorption from L-130 stands out. The amount of caffeine permeated from the L-130 sample is approximately twice larger than from H-series samples, Figure 7C, 7D. The higher efficiency of sample L-130 is assumed to be caused by its physical properties, namely the lowest elasticity among all tested materials. While more elastic H-series samples tend to keep their original shape on uneven skin surface, the L-130 adheres to the skin considerably better, see comparison of L-130 and H-130 hydrogel in Figure 8. Because adherence to the skin is one of the key qualities dictating effectiveness of transdermal absorption, [4] this observation readily explain the improved transdermal delivery of caffeine from L-130 sample.

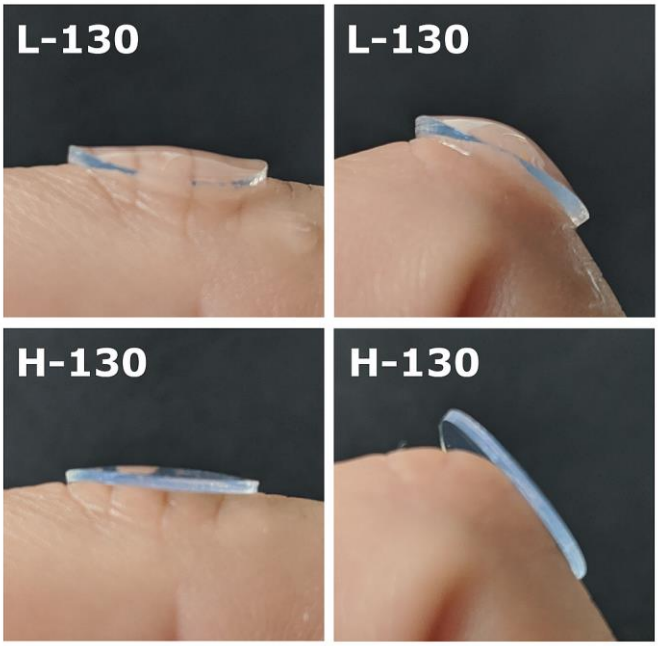

Figure 8: The comparison of L-130 and H-130 hydrogels on the uneven skin surface.

The hydrogel L-130 is thus assumed to be the most promising candidate for transdermal administration of biologically active substances of all tested materials without using any skin-penetration enhancers.

4. CONCLUSION

The combination of different concentration of crosslinker, 2,3-dialdehyde cellulose, DAC, and different molecular weight of the matrix, poly(vinyl alcohol), PVA, was used to optimize the properties of thin PVA/DAC hydrogel films towards topical applications. While changing the amount of crosslinker is a standard method for tuning the properties of hydrogels, simultaneous change of the molecular weight of the second hydrogel component provides another, yet often overlooked, degree of freedom which may be exploited to obtain

the material with specific properties. Detailed analysis revealed that increased M_w of PVA influences hydrogel network parameters at (macro)molecular level (crosslink density, mesh size) providing additional stabilization. Impact of these molecular-scale changes on bulk properties of hydrogels was largest for equilibrium swelling capacity, viscoelastic characteristics and it also notably improved physical properties of L-130 films compared to L-31 (L-130 samples did not disintegrate during handling unlike the L-31). On the other hand, the specific surface area and total pore volume of lyophilized samples is governed by the amount of crosslinker and does not depend on the type of PVA, which however influences the mean pore size. Neither the amount of crosslinker or the molecular weight of PVA has a significant influence on drug release rates, likely because the role of hydrogel network density does not manifest in thin-film formulations. All hydrogels were non-cytotoxic under *in vitro* conditions, they did not affect the cellular growth and cell morphology or support the adherence of cells to their surface, which imply their suitability as biomaterials for transdermal drug delivery and wound dressings.

The best candidate for preparation of dermal patches and masks intended for transdermal delivery of biologically-active compounds is the hydrogel L-130 prepared using higher-molecular weight PVA matrix in combination with a lower concentration of crosslinker. It has high porosity and high water content (related to drug-loading capacity), physical properties allowing easy handling and best adherence to the skin from all tested samples, which enhanced its transdermal drug delivery properties. Conversely, a combination of higher M_w of PVA and a higher concentration of crosslinker leads to more elastic hydrogels with a denser network.

ACKNOWLEDGEMENT

This work was supported by the Ministry of Education, Youth and Sports of the Czech Republic Program NPU I (LO1504). M.M. was supported by the internal grant for specific research from TBU in Zlín no. IGA/CPS/2020/003.

Competing interest: The authors declare no competing financial or other interest.

REFERENCES

[1] E. Caló, V.V. Khutoryanskiy, Biomedical applications of hydrogels: A review of patents and commercial products, European Polymer Journal. 65 (2015) 252–267. https://doi.org/10.1016/j.eurpolymj.2014.11.024.

[2] G.D. Winter, Formation of the Scab and the Rate of Epithelization of Superficial Wounds in the Skin of the Young Domestic Pig, Nature. 193 (1962) 293–294. https://doi.org/10.1038/193293a0.

[3] E.A. Kamoun, E.-R.S. Kenawy, X. Chen, A review on polymeric hydrogel membranes for wound dressing applications: PVA-based hydrogel dressings, J Adv Res. 8 (2017) 217–233. https://doi.org/10.1016/j.jare.2017.01.005.

[4] M.E. Parente, A.O. Andrade, G. Ares, F. Russo, Á. Jiménez- Kairuz, Bioadhesive hydrogels for cosmetic applications, International Journal of Cosmetic Science. 37 (2015) 511–518. https://doi.org/10.1111/ics.12227.
[5] H. Ruan, Q. Hu, D. Wen, Q. Chen, G. Chen, Y. Lu, J. Wang, H. Cheng, W. Lu, Z. Gu, A Dual-Bioresponsive Drug-Delivery Depot for Combination of Epigenetic Modulation and Immune Checkpoint Blockade, Advanced Materials. 31 (2019) 1806957. https://doi.org/10.1002/adma.201806957.
[6] C. Wang, J. Wang, X. Zhang, S. Yu, D. Wen, Q. Hu, Y. Ye, H. Bomba, X. Hu, Z. Liu, G. Dotti, Z. Gu, In situ formed reactive oxygen species–responsive scaffold with gemcitabine and checkpoint inhibitor for combination therapy, Science Translational Medicine. 10 (2018). https://doi.org/10.1126/scitranslmed.aan3682.
[7] J.K. Li, N. Wang, X.S. Wu, Poly(vinyl alcohol) nanoparticles prepared by freezing–thawing process for protein/peptide drug delivery, Journal of Controlled Release. 56 (1998) 117–126. https://doi.org/10.1016/S0168-3659(98)00089-3.
[8] S.-H. Hyon, W.-I. Cha, Y. Ikada, M. Kita, Y. Ogura, Y. Honda, Poly(vinyl alcohol) hydrogels as soft contact lens material, Journal of Biomaterials Science, Polymer Edition. 5 (1994) 397–406. https://doi.org/10.1163/156856294X00103.
[9] U.-J. Kim, S. Kuga, M. Wada, T. Okano, T. Kondo, Periodate Oxidation of Crystalline Cellulose, Biomacromolecules. 1 (2000) 488–492. https://doi.org/10.1021/bm0000337.
[10] L. Münster, J. Vícha, J. Klofáč, M. Masař, P. Kucharczyk, I. Kuřitka, Stability and aging of solubilized dialdehyde cellulose, Cellulose. 24 (2017) 2753–2766. https://doi.org/10.1007/s10570-017-1314-x.
[11] U.-J. Kim, M. Wada, S. Kuga, Solubilization of dialdehyde cellulose by hot water, Carbohydrate Polymers. 56 (2004) 7–10. https://doi.org/10.1016/j.carbpol.2003.10.013.
[12] I. Sulaeva, K.M. Klinger, H. Amer, U. Henniges, T. Rosenau, A. Potthast, Determination of molar mass distributions of highly oxidized dialdehyde cellulose by size exclusion chromatography and asymmetric flow field-flow fractionation, Cellulose. 22 (2015) 3569–3581. https://doi.org/10.1007/s10570-015-0769-x.
[13] J.A. Sirviö, H. Liimatainen, M. Visanko, J. Niinimäki, Optimization of dicarboxylic acid cellulose synthesis: Reaction stoichiometry and role of hypochlorite scavengers, Carbohydrate Polymers. 114 (2014) 73–77. https://doi.org/10.1016/j.carbpol.2014.07.081.
[14] G. Yan, X. Zhang, M. Li, X. Zhao, X. Zeng, Y. Sun, X. Tang, T. Lei, L. Lin, Stability of Soluble Dialdehyde Cellulose and the Formation of Hollow Microspheres: Optimization and Characterization, ACS Sustainable Chem. Eng. 7 (2019) 2151–2159. https://doi.org/10.1021/acssuschemeng.8b04825.
[15] H. Liimatainen, M. Visanko, J.A. Sirviö, O.E.O. Hormi, J. Niinimaki, Enhancement of the Nanofibrillation of Wood Cellulose through Sequential Periodate–Chlorite Oxidation, Biomacromolecules. 13 (2012) 1592–1597. https://doi.org/10.1021/bm300319m.
[16] U.-J. Kim, Y.R. Lee, T.H. Kang, J.W. Choi, S. Kimura, M. Wada, Protein adsorption of dialdehyde cellulose-crosslinked chitosan with high amino group contents, Carbohydrate Polymers. 163 (2017) 34–42. https://doi.org/10.1016/j.carbpol.2017.01.052.
[17] L. Münster, J. Vícha, J. Klofáč, M. Masař, A. Hurajová, I. Kuřitka, Dialdehyde cellulose crosslinked poly(vinyl alcohol) hydrogels: Influence of catalyst and crosslinker shelf life, Carbohydrate Polymers. 198 (2018) 181–190. https://doi.org/10.1016/j.carbpol.2018.06.035.
[18] L. Münster, Z. Capáková, M. Fišera, I. Kuřitka, J. Vícha, Biocompatible dialdehyde cellulose/poly(vinyl alcohol) hydrogels with tunable properties, Carbohydrate Polymers. 218 (2019) 333–342. https://doi.org/10.1016/j.carbpol.2019.04.091.

[19] A. Ganeshpurkar, A.K. Saluja, The Pharmacological Potential of Rutin, Saudi Pharmaceutical Journal. 25 (2017) 149–164. https://doi.org/10.1016/j.jsps.2016.04.025.
[20] N.Q. Tran, Y.K. Joung, E. Lih, K.D. Park, In Situ Forming and Rutin-Releasing Chitosan Hydrogels As Injectable Dressings for Dermal Wound Healing, Biomacromolecules. 12 (2011) 2872–2880. https://doi.org/10.1021/bm200326g.
[21] J.K. Choi, S.-H. Kim, Rutin suppresses atopic dermatitis and allergic contact dermatitis, Exp Biol Med (Maywood). 238 (2013) 410–417. https://doi.org/10.1177/1535370213477975.
[22] L. Luo, M.E. Lane, Topical and transdermal delivery of caffeine, International Journal of Pharmaceutics. 490 (2015) 155–164. https://doi.org/10.1016/j.ijpharm.2015.05.050.
[23] S. Trauer, A. Patzelt, N. Otberg, F. Knorr, C. Rozycki, G. Balizs, R. Büttemeyer, M. Linscheid, M. Liebsch, J. Lademann, Permeation of topically applied caffeine through human skin – a comparison of in vivo and in vitro data, Br J Clin Pharmacol. 68 (2009) 181–186. https://doi.org/10.1111/j.1365-2125.2009.03463.x.
[24] P. Engel, L. Hein, A.C. Spiess, Derivatization-free gel permeation chromatography elucidates enzymatic cellulose hydrolysis, Biotechnology for Biofuels. 5 (2012) 77. https://doi.org/10.1186/1754-6834-5-77.
[25] L. Münster, B. Hanulíková, M. Machovský, F. Latečka, I. Kuřitka, J. Vícha, Mechanism of sulfonation-induced chain scission of selectively oxidized polysaccharides, Carbohydrate Polymers. 229 (2020) 115503. https://doi.org/10.1016/j.carbpol.2019.115503.
[26] P.J. Flory, J. Rehner, Statistical Mechanics of Cross- Linked Polymer Networks II. Swelling, The Journal of Chemical Physics. 11 (1943) 521–526. https://doi.org/10.1063/1.1723792.
[27] N.A. Peppas, E.W. Merrill, Determination of interaction parameter χ1, for poly(vinyl alcohol) and water in gels crosslinked from solutions, J. Polym. Sci. Polym. Chem. Ed. 14 (1976) 459–464. https://doi.org/10.1002/pol.1976.170140216.
[28] S.K. H. Gulrez, S. Al-Assaf, G. O, Hydrogels: Methods of Preparation, Characterisation and Applications, in: A. Carpi (Ed.), Progress in Molecular and Environmental Bioengineering - From Analysis and Modeling to Technology Applications, InTech, 2011. https://doi.org/10.5772/24553.
[29] B.J. Tighe, The Role of Permeability and Related Properties in the Design of Synthetic Hydrogels for Biomedical Applications, Brit. Poly.J. 18 (1986) 8–13. https://doi.org/10.1002/pi.4980180104.
[30] N.A. Peppas, Y. Huang, M. Torres-Lugo, J.H. Ward, J. Zhang, Physicochemical Foundations and Structural Design of Hydrogels in Medicine and Biology, Annu. Rev. Biomed. Eng. 2 (2000) 9–29. https://doi.org/10.1146/annurev.bioeng.2.1.9.
[31] H. Omidian, S.-A. Hasherni, F. Askari, S. Nafisi, Swelling and Crosslink Density Measurements for Hydrogels, (n.d.) 6.
[32] M. Dias, A. Farinha, E. Faustino, J. Hadgraft, J. Pais, C. Toscano, Topical delivery of caffeine from some commercial formulations, International Journal of Pharmaceutics. 182 (1999) 41–47. https://doi.org/10.1016/S0378-5173(99)00067-8.
[33] F. Bonina, S. Bader, L. Montenegro, C. Scrofani, M. Visca, Three phase emulsions for controlled delivery in the cosmetic field, International Journal of Cosmetic Science. 14 (1992) 65–74. https://doi.org/10.1111/j.1467-2494.1992.tb00040.x.
[34] M.J. Santander-Ortega, T. Stauner, B. Loretz, J.L. Ortega-Vinuesa, D. Bastos-González, G. Wenz, U.F. Schaefer, C.M. Lehr, Nanoparticles made from novel starch derivatives for transdermal drug delivery, Journal of Controlled Release. 141 (2010) 85–92. https://doi.org/10.1016/j.jconrel.2009.08.012.

[35] M. Pilloni, G. Ennas, M. Casu, A.M. Fadda, F. Frongia, F. Marongiu, R. Sanna, A. Scano, D. Valenti, C. Sinico, Drug silica nanocomposite: preparation, characterization and skin permeation studies, Pharmaceutical Development and Technology. 18 (2013) 626–633. https://doi.org/10.3109/10837450.2011.653821.

Graphical abstract:

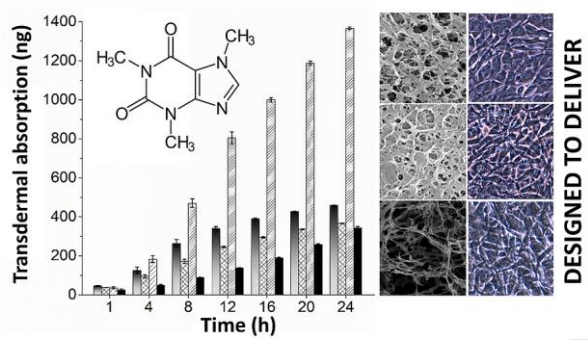

Author_roles

Monika Muchová : Investigation, Visualization, Formal analysis, Writing, Lukáš Münster: Investigation, Visualization, Writing, Zdenka Capáková: Investigation Veronika Mikulcová : Investigation, Ivo Kuřitka: Resources, Funding acquisition, Jan Vícha : Conceptualization, Writing, Supervision

Declaration of interests

☒ The authors declare that they have no known competing financial interests or personal relationships that could have appeared to influence the work reported in this paper.

☐The authors declare the following financial interests/personal relationships which may be considered as potential competing interests:

Highlights

- Dialdehydecellulose/PVA films designed for transdermal drug-delivery applications
- Green synthesis, biocompatible, improved transdermal drug-delivery
- Molecular weight of PVA used to fine-tune the hydrogel properties